frontiers in Chemistry

ORIGINAL RESEARCH
published: 29 November 2021
doi: 10.3389/fchem.2021.740140

High Loading Capacity and Wear Resistance of Graphene Oxide/Organic Molecule Assembled Multilayer Film

Li Chen[1], *Gang Wu*[1], *Yin Huang*[1], *Changning Bai*[2,3], *Yuanlie Yu*[2,3] *and Junyan Zhang*[2,3]*

[1]School of Petrochemical Technology, Lanzhou University of Technology, Lanzhou, China, [2]Key Laboratory of Science and Technology on Wear and Protection of Materials, Lanzhou Institute of Chemical Physics, Chinese Academy of Sciences, Lanzhou, China, [3]Center of Materials Science and Optoelectronics Engineering, University of Chinese Academy of Sciences, Beijing, China

Taking advantage of the strong charge interactions between negatively charged graphene oxide (GO) sheets and positively charged poly(diallyldimethylammonium chloride) (PDDA), self-assembled multilayer films of $(GO/PDDA)_n$ were created on hydroxylated silicon substrates by alternating electrostatic adsorption of GO and PDDA. The formation and structure of the films were analyzed by means of water contact angle measurement, thickness measurement, atomic force microscopy (AFM) and X-ray photoelectron spectroscopy (XPS). Meanwhile, tribological behaviors in micro- and macro- scale were investigated by AFM and a ball-on-plate tribometer, respectively. The results showed that $(GO/PDDA)_n$ multilayer films exhibited excellent friction-reducing and anti-wear abilities in both micro- and macro-scale, which was ascribed to the special structure in $(GO/PDDA)_n$ multilayer films, namely, a well-stacked GO–GO layered structure and an elastic 3D crystal stack in whole. Such a film structure is suitable for design molecular lubricants for MEMS and other microdevices.

Keywords: 2D materials, self-assembly, composite films, micro/macro-tribological behaviors, high loading capacity

OPEN ACCESS

Edited by:
Andreas Rosenkranz, University of Chile, Chile

Reviewed by:
Xiaolong Zhu, Merck, United States
Manishkumar Ramesh Shimpi, Stockholm University, Sweden

***Correspondence:**
Junyan Zhang
zhangjunyan@licp.cas.cn

Specialty section:
This article was submitted to Solid State Chemistry, a section of the journal Frontiers in Chemistry

Received: *14 July 2021*
Accepted: *26 October 2021*
Published: *29 November 2021*

Citation:
Chen L, Wu G, Huang Y, Bai C, Yu Y and Zhang J (2021) High Loading Capacity and Wear Resistance of Graphene Oxide/Organic Molecule Assembled Multilayer Film. Front. Chem. 9:740140. doi: 10.3389/fchem.2021.740140

INTRODUCTION

The advances in micro-nano manufacturing technology have promoted the rapid development of microelectronic mechanical systems (MEMS) and micro/nanodevices. Due to the decrease in component size and the enhancement of surface effect, stiction, friction, and wear became significant barriers for the successful development of durable and reliable MEMS (Maboudian and Carraro, 2004; Shen and Meng, 2013). Therefore, it is very urgent to design and construct micro-nano self-lubricating system, which can improve the tribological properties between contacting surfaces on micro- and nanoscales. Molecular lubricants, because of the simple preparation method, controllable structure, high stability, and good self-recovery, are considered to be prospective candidates to resolve the tribological problems of MEMS over the last decades (Liu et al., 2012; Chen et al., 2014a; Liang et al., 2015; Cao et al., 2018). However, the inherent low loading capacity of organic molecular lubricants makes them scarcely meet the needs of long-term stability and high reliability for MEMS (Song et al., 2008; Ou et al., 2009; Chen et al., 2016). Therefore, it is desired to design and construct organic molecule films with inorganic materials such as two dimensional (2D) materials acted as steel in concrete so as to enhance the loading capacity of organic molecule films.

With excellent mechanical strength, low friction, and high chemical stability, graphene is expected to reduce the adhesion, friction, and wear problems of MEMS as a solid lubricant (Lee et al., 2008; Popov et al., 2013; Berman et al., 2014). If graphene is introduced into self-assembled films, it cannot

only enhance the tribological properties of self-assembled films but also improve the loading capacity of the molecular films. However, the ideal graphene material is inert, which makes it difficult to build a powerful bond with other surfaces (Ramanathan et al., 2008; Li et al., 2019). With layer structure and some similar properties to graphene, graphene oxide (GO) and reduced graphene oxide (RGO) films may be good solid lubricants to MEMS (Mi et al., 2012; Li et al., 2013; Liang et al., 2013). GO has various active functional groups, including hydroxyl, carboxyl, and epoxy groups (Guex et al., 2017); therefore, 2D GO sheets can chemically adsorb on a variety of substrates (Mi et al., 2012; Li et al., 2013). Moreover, 2D GO sheets can be combined with organic molecular precursors to construct multilayer films *via* covalent interaction (Cassagneau et al., 2000; Ou et al., 2012; Mungse et al., 2016). Self-assembly technique is useful to prepare organic molecule films with GO. Taking advantage of the chemical reactions between epoxy/carboxyl and amine groups, GO sheets were covalently attached onto Si substrates modified by self-assembled monolayer of (3-aminopropyl) triethoxysilane (APTES SAM) (Ou et al., 2010). After thermal reduction of APTES-GO, the obtained APTES-RGO film exhibited excellent friction-reducing and anti-wear performances under low applied loads. APTES-RGO nanolayer assembled on the surface of Ti or titanium alloy substrates also holds remarkable tribological properties in nano/micro scale (Li et al., 2013; Li et al., 2019). Octadecyltrichlorosilane (OTS), a hydrophobic alkylsilane, was assembled onto the GO surface of APTES-GO layer *via* C–O–Si bonding (Ou et al., 2011). It has demonstrated that the OTS outer layer could reduce the adhesion/friction greatly, and the obtained APTES–GO–OTS multilayer film showed improved tribological performances than the APTES–GO layer. However, the loading capacity and anti-wear life of these films were still not satisfactory.

Poly(diallyldimethylammonium chloride) (PDDA), a kind of polymer with excellent stability, can be easily inserted by different methods between GO lamellae to form intercalated GO composites (Ni et al., 2010). As a novel overcoating layer for flexible transparent conductive films, this mechanically stable ultrathin film with multilayered GO and PDDA could protect silver nanowires from friction (Lee et al., 2015). Herein, 2D GO nanosheets with negative charge and PDDA with positive charge were employed to construct mechanically stable $(GO/PDDA)_n$ multilayer films by a layer-by-layer (LBL) self-assembly method. In this report, we focus on the tribological behaviors of $(GO/PDDA)_n$ multilayers in micro- and macro-scales. The combination of elastically strong PDDA and mechanically strong 2D GO nanosheets is expected to boost high loading capacity and anti-wear life, aiming at developing thin-film lubricants suitable for MEMS and micro/nanodevices.

EXPERIMENTAL SECTION

Materials

Natural graphite powder was obtained from Qingdao Huatai Lubricating and Sealing Technology Co., Ltd. N-type polished single-crystal silicon (100) wafers were purchased from MCL Electronic Materials Co., Ltd. Poly(diallyldimethylammonium chloride) solution (PDDA, Mw: 100,000–200,000, 20 wt%) was purchased from Sigma-Aldrich and used as received. The chemical structures of GO and PDDA are shown in **Figure 1A**. Ultrapure water (>18 MΩ) was used throughout the experiment.

Preparation of graphene oxide

Natural flake graphite powder (1.0 g) and $NaNO_3$ (1.0 g) were mixed with 98% H_2SO_4 (50 ml) in an ice bath. $KMnO_4$ (6.0 g) was slowly added to the suspension with stirring to keep the temperature below 10°C. Then the mixture was kept at 35°C and stirred for 4 h in a water bath. Subsequently, ultrapure water (100 ml) was gradually added with vigorous stirring. The reaction temperature increased rapidly and kept at 98°C for 15 min by heating. Then, the mixture was further treated with 30% H_2O_2 (40 ml). After cooling to room temperature, the mixture was centrifuged and washed with 5% HCl and then deionized water for several times. Water-soluble GO was obtained.

Fabrication of self-assembled films

Silicon wafers were hydroxylated in Piranha solution (mixture of 7:3 (v/v) 98% H_2SO_4 and 30% H_2O_2) at 90°C for 30 min. After being thoroughly rinsed with ultrapure water and blown dry with N_2, the hydroxylated silicon wafers were immersed into the GO aqueous solution at 80°C for 12 h. Then the wafers were ultrasonically cleaned in ultrapure water and blown dry with N_2 gas, and the film was designated as GO SAM. Subsequently, GO SAM covered Si wafers were kept in the PDDA water solution (1.5 wt%) for 1 h, followed by washing with ultrapure water and drying in N_2 gas. The obtained sample was designated as $(GO/PDDA)_1$. Repeating above operation three and five times, respectively, the obtained samples were coded as $(GO/PDDA)_3$ and $(GO/PDDA)_5$. As a contrast, PDDA SAM was prepared by keeping hydroxylated silicon wafers in PDDA solution for 1 h and then treated using the above washing and drying steps.

Characterization

The zeta potentials of GO and PDDA in water solution were measured with a Zetasizer Nano Series instrument (Malvern Instruments Ltd., UK) at 25°C. Water contact angles (WCA) of the samples were characterized by a contact angle meter (SZ-CAM). The reported data are average values of at least five repeated measurements for each sample. The film thicknesses were measured on a L116-E ellipsometer (Gaertner, MN, USA) equipped with a He–Ne laser (632.8 nm) at an incident angle of 50°. A refractive index of 1.46 was set for silicon oxide and 1.45 for GO, PDDA, and $(GO/PDDA)_n$ layers. Raman spectra were collected by a Raman spectrometer (LabRAM HR 800, Horiba Jobin Yvon). X-ray photoelectron spectroscopy (XPS, Kratos Axis Ultra DLD) was employed to analyze the chemical composition and element chemical state on specimen surfaces. The surface morphologies of the samples were observed by a Nanoscope IIIa Multimode atomic force microscope (AFM, Digital Instruments, UK) in tapping mode.

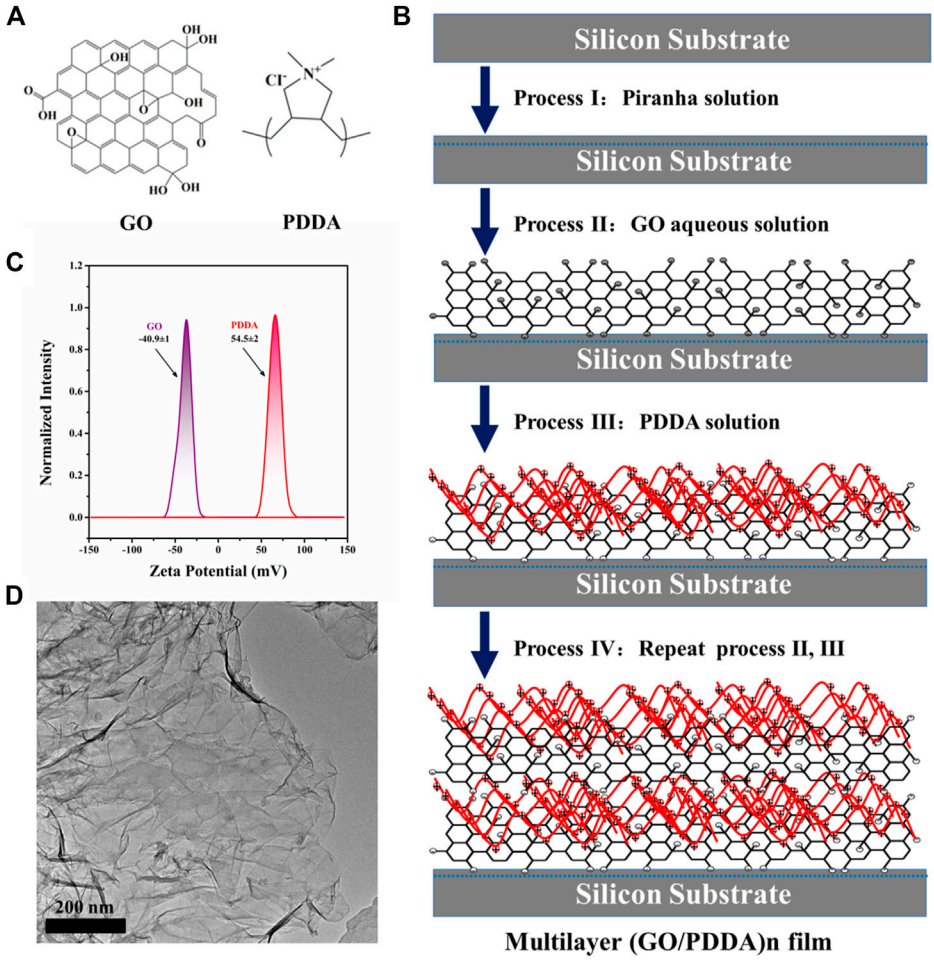

FIGURE 1 | (A) Molecular structures of graphene oxide (GO) and poly(diallyldimethylammonium chloride) (PDDA), **(B)** Schematic illustration of the constructing process of $(GO/PDDA)_n$ multilayer films by layer-by-layer (LBL) self-assembly method, **(C)** ζ potential for GO and PDDA materials, **(D)** TEM image of GO material.

Friction tests

Microtribological properties of the films were investigated by a Nanoscope IIIa Multimode scanning probe microscope in contact mode. V-shape Si_3N_4 cantilever with an announced elastic force constant of 2 N/m was used. The output voltages were directly used as the relative friction forces. The friction force–load curve was made from the friction loops. At least six separate locations on each sample were selected for measurement. The adhesive force of each specimen was an average value of at least six locations on each sample surface. All experiments were carried out under ambient conditions of 20°C and 40%–50% relative humidity.

A UMT-2MT tribometer (CETR, USA) in a ball-on-plate reciprocating mode was employed to evaluate the macrotribological performance. Si_3N_4 ball ($\Phi = 3$ mm) used as upper counterpart was stationary, while the lower specimen adhered on the flat base kept reciprocating at a distance of 5 mm. The loads of 0.1, 0.2, 0.3, and 0.4 N were applied for the measurements. At least three repeated tests were performed for each specimen. All tests were made under ambient conditions of 20°C and 40%–50% relative humidity.

RESULTS AND DISCUSSION

Formation and characterization of (graphene oxide/ poly(diallyldimethylammonium chloride)$_n$ film

Self-assembled multilayer films of $(GO/PDDA)_n$ were created on silicon wafers by alternating electrostatic adsorption of GO and PDDA, and the constructing process is shown schematically in **Figure 1B**. As illustrated, GO sheets were introduced onto the hydroxylated silicon wafers to create an underlayer. GO sheets can be chemisorbed onto hydroxylated silicon substrates *via* chemical reactions between hydroxyl/carboxyl and hydroxyl groups. Then negatively charged GO layer was modified by electrostatic adsorption of positively charged PDDA. The

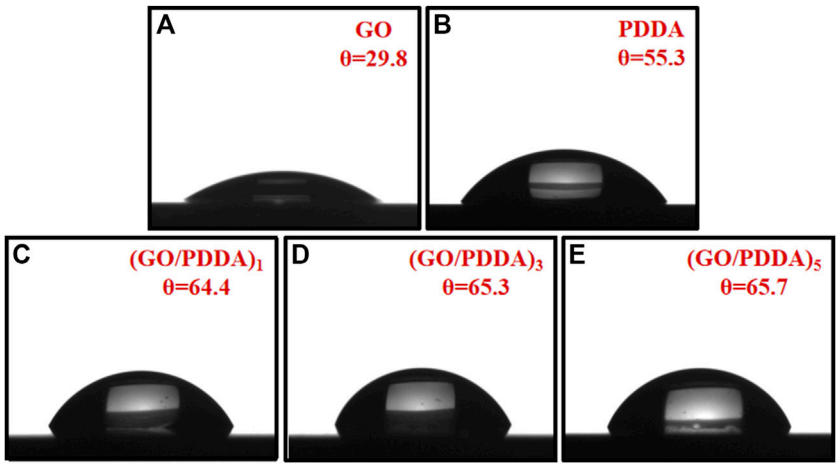

FIGURE 2 | Water contact angles (WCA) of composite films.

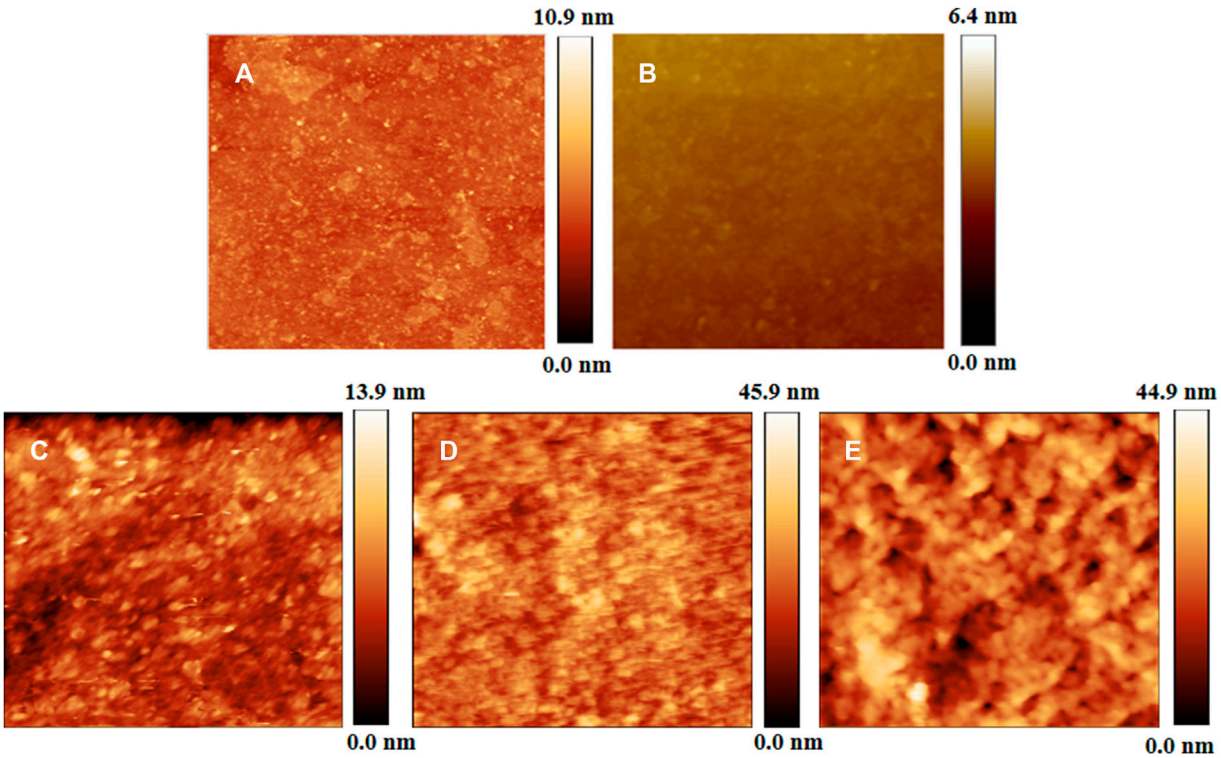

FIGURE 3 | Atomic force microscope (AFM) morphologies of GO self-assembled monolayer (SAM) **(A)**, PDDA SAM **(B)**, $(GO/PDDA)_1$ **(C)**, $(GO/PDDA)_3$ **(D)**, and $(GO/PDDA)_5$ **(E)** over a scanning area of 2.5 μm × 2.5 μm.

strong charge interactions sustain the GO/PDDA bilayers and maintain them during this LBL process (Qureshi et al., 2013), which was evidenced by the **Figure 1C**. The target film designated as $(GO/PDDA)_1$, thus, was formed. Alternating electrostatic adsorption of GO sheets and PDDA three and five times, respectively, the multilayer films of $(GO/PDDA)_3$ and $(GO/PDDA)_5$ were obtained. It is worth noting that the preparation of the composite film is also derived from the good film-forming properties of graphene oxide, as shown in **Figure 1D**. Furthermore, the ability to control the thickness using the LBL method is evaluated. The film thicknesses were measured using ellipsometer (Porter et al., 1987), in which their thicknesses are, respectively 3.37, 9.41, and 15.93 nm for the $(GO/PDDA)_1$, $(GO/PDDA)_3$, and $(GO/PDDA)_5$ layers. It

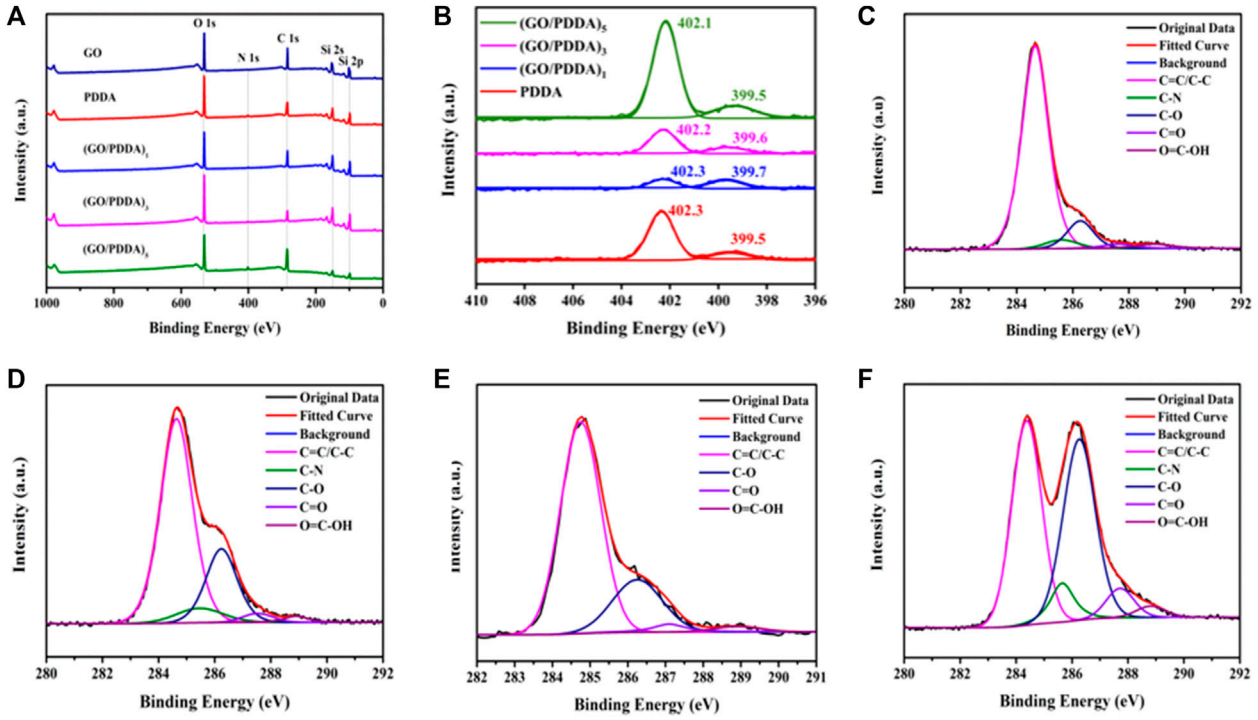

FIGURE 4 | X-ray photoelectron spectroscopy (XPS) survey spectra for different samples **(A)**, N 1s spectra for PDDA film and $(GO/PDDA)_n$ films **(B)**, C 1s spectra for GO material **(C)**, $(GO/PDDA)_1$ **(D)**, $(GO/PDDA)_3$ **(E)**, $(GO/PDDA)_5$ **(F)**.

can be seen that the growth of the $(GO/PDDA)_n$ films was linear.

Contact angle meter was applied to determine the surface wettability of the films, as shown in **Figure 2**. The WCA for silicon wafers after the hydroxylation process is less than 5°, which agrees with the reported results (Song et al., 2008; Ou et al., 2010). GO and PDDA are known as hydrophilic materials because of the oxygen-containing groups and the quaternary ammonium salt segments. The WCAs for GO SAM and PDDA SAM were 29.8° and 55.3°, respectively. The films showed similar WCA values of 64.4°, 65.3°, and 65.7° for $(GO/PDDA)_1$, $(GO/PDDA)_3$, and $(GO/PDDA)_5$ layers, respectively. Compared with PDDA SAM, $(GO/PDDA)_n$ multilayers with the topmost PDDA exhibited higher hydrophobicity. That is attributed to the strong interaction between the quaternary ammonium salt segments of PDDA and the anionic functional groups of GO, which expose the hydrophobic backbone of the topmost PDDA to the surface (Lee et al., 2015).

The AFM morphology in **Figure 3A** shows that the irregular GO sheets were discontinuously distributed on Si substrate. PDDA SAM is relatively smooth with the root-mean-square (RMS) microroughness of about 1.29 nm over a scanning range of 2.5 μm × 2.5 μm, while the $(GO/PDDA)_n$ films are composed of plentiful regular grains, and the surfaces are relatively rough with the RMS microroughnesses of about 1.76, 3.04, and 4.70 nm for the $(GO/PDDA)_1$, $(GO/PDDA)_3$, and $(GO/PDDA)_5$ layers, respectively.

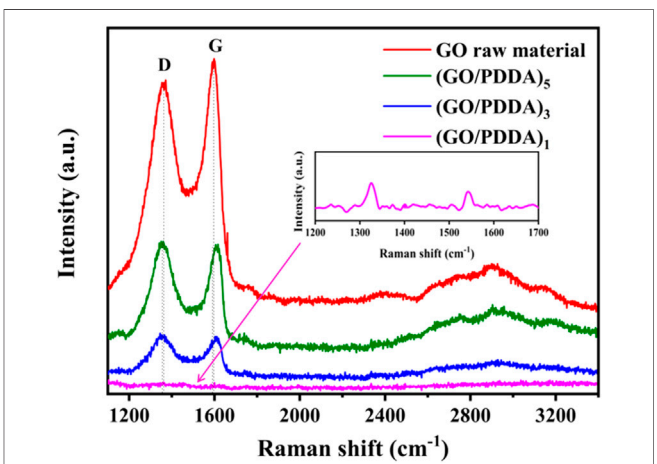

FIGURE 5 | Raman spectra of GO material and $(GO\text{-}PDDA)_n$ films.

XPS was employed to analyze the detailed composition and the element chemical status of the as-prepared films (**Figure 4**). The N 1s peak at 400.1 eV in the spectrum of PDDA indicated that PDDA was successfully assembled on silicon surface (**Figures 4A, B**). In all spectra of $(GO/PDDA)_n$ films, the N 1s signals centered at 400.1 eV indicated the successful covalent attachment of PDDA on GO layer. The fine spectrum of C 1s region of GO layer (**Figure 4C**) was deconvoluted into C=C/C–C,

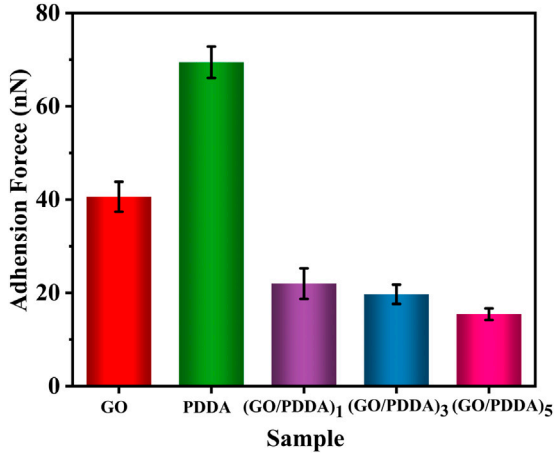

FIGURE 6 | Adhesive forces for different samples.

C–O, C=O, and O=C-OH bands at 284.8, 286.3, 287.1, and 288.9 eV, respectively (Yang et al., 2009; Stankovich et al., 2007; Tang et al., 2009). C 1s spectrum of $(GO/PDDA)_1$ film in **Figure 4D** could be fitted to five bands at 284.7, 285.6, 286.3, 287.6, and 288.9 eV, which were attributed to C=C/C–C, C–N, C–O, C=O, and O=C–OH groups, respectively. C 1s spectra of $(GO/PDDA)_3$ and $(GO/PDDA)_5$ films (**Figures 4E, F**) could be deconvoluted into the same bands as that of $(GO/PDDA)_1$ film. The content of C–N from the C 1s fitting results was 4.11%, 6.66%, and 7.30% for $(GO/PDDA)_1$, $(GO/PDDA)_3$, and $(GO/PDDA)_5$ films, respectively. The content of C-N increases with the increasing number of $(GO\text{-}PDDA)_n$ layers, which indicated that PDDA and GO could form an electrostatic interaction (Lee et al., 2015) in $(GO/PDDA)_n$ films.

Figure 5 shows the Raman spectra of GO and $(GO/PDDA)_n$ films. Clearly the D peak that appeared at ~1,350 cm^{-1} and the G peak that appeared at ~1,590 cm^{-1} are the primary features of the Raman spectrum for GO sheets (Tan et al., 2004). The D and G peaks for the $(GO/PDDA)_1$ layer were almost invisible, while the $(GO/PDDA)_3$ and $(GO/PDDA)_5$ layers exhibited clear D and G peaks at about 1,355 and 1,605 cm^{-1}, respectively. As the number of $(GO\text{-}PDDA)_n$ layers increases, the intensity of the D and G bands increased, and the peaks of the D and G bands became sharper. It means that a well-stacked GO–GO-layered structure was still maintained in $(GO/PDDA)_n$ layer (Ni et al., 2010; Lee et al., 2015). Moreover, the sliding phenomenon between the GO sheets separated by PDDA appears to dominate as increasing $(GO/PDDA)_n$ layers (Lee et al., 2015).

Microtribological behaviors

Figure 6 presents the adhesive forces between the AFM tip and the sample surfaces. Strong adhesions were observed on the surfaces of GO layer and PDDA SAM. The adhesive force is closely related to the water contact angle (**Figure 2**). The surface with higher hydrophobicity exhibits lower adhesion because the adhesion is mainly dominated by capillary force between the AFM tip and the sample surface (Ou et al., 2009). Compared with PDDA SAM, $(GO/PDDA)_n$ multilayers possessed the better adhesion-resistance performance. Moreover, the $(GO/PDDA)_n$ films with the topmost PDDA showed similar adhesive forces.

The cantilever deflection voltage caused by friction is proportional to the actual friction force in AFM testing, so the output voltage signal is used as the friction force (**Figure 7A**). In general, adhesive force is an important factor in controlling the friction behavior. Decreasing adhesion is conducive to reducing friction forces of self-assembled films on microscale (Ou et al., 2011; Chen et al., 2014b; Chen et al., 2016). $(GO/PDDA)_n$ films with the topmost PDDA showed lower friction force than PDDA SAM due to the higher hydrophobicity and lower adhesive force of $(GO/PDDA)_n$ films. With the increasing number of $(GO/PDDA)_n$ layers, $(GO/PDDA)_n$ films exhibited higher friction force because of the larger roughness. Moreover, the profiles of friction force versus external loads are approximately linear, which can be well fitted by Amonton's law:

$$F_L = \mu F_N + F_0 \quad (1)$$

where F_L is the friction force, μ is friction coefficient, F_N is the normal force, and F_0 is the friction force when the normal force is zero (Chen et al., 2014b; Foster et al., 2006; Houston et al., 2005). It is clearly obtained that both GO SAM and PDDA SAM possess high relative friction coefficients, while the $(GO/PDDA)_n$ multilayer films exhibit much better lubricity (**Figure 7B**). It can be attributed to the higher hydrophobicity of the $(GO/PDDA)_n$ multilayer films, which plays an important part in reducing adhesive force between AFM tip and film surface. Many researchers have found that the friction would decrease with the reducing adhesion (Houston et al., 2005; Foster et al., 2006; Ou et al., 2011; Chen et al., 2014b; Chen et al., 2016).

Macrotribological behaviors

The wear resistance is an important factor for lubricant films. The macrotribological behaviors of the prepared films were evaluated by a ball-on-plate tribometer, and the results are shown in **Figure 8**. The GO layer showed poor tribological properties and very short anti-wear life. For PDDA SAM, the friction coefficient is about 0.3 under the loads of 0.1 and 0.2 N (**Figures 8A, B**). PDDA SAM was worn out quickly under the load of 0.3 N (**Figure 8C**). It means that the load-carry capacity of PDDA SAM is poor. In contrast, $(GO/PDDA)_n$ multilayer films exhibited excellent friction-reducing and anti-wear abilities. The friction coefficients of $(GO/PDDA)_n$ films are lower than that of PDDA SAM in all the applied loads, and the friction coefficients of multilayer films show a gradual decrease as the increasing number of $(GO/PDDA)_n$ layers. Besides, the $(GO/PDDA)_n$ films possessed higher load-carrying capacity. Under the conditions of 0.4 N and 1 Hz, they showed anti-wear life of more than 11,800, 14,600, and 16,600 s for the $(GO/PDDA)_1$, $(GO/PDDA)_3$, and $(GO/PDDA)_5$ layers, respectively (**Figure 8D**). The excellent lubricity can be attributed to the special structure in $(GO/PDDA)_n$ multilayer films. PDDA enlarge GO sheets to

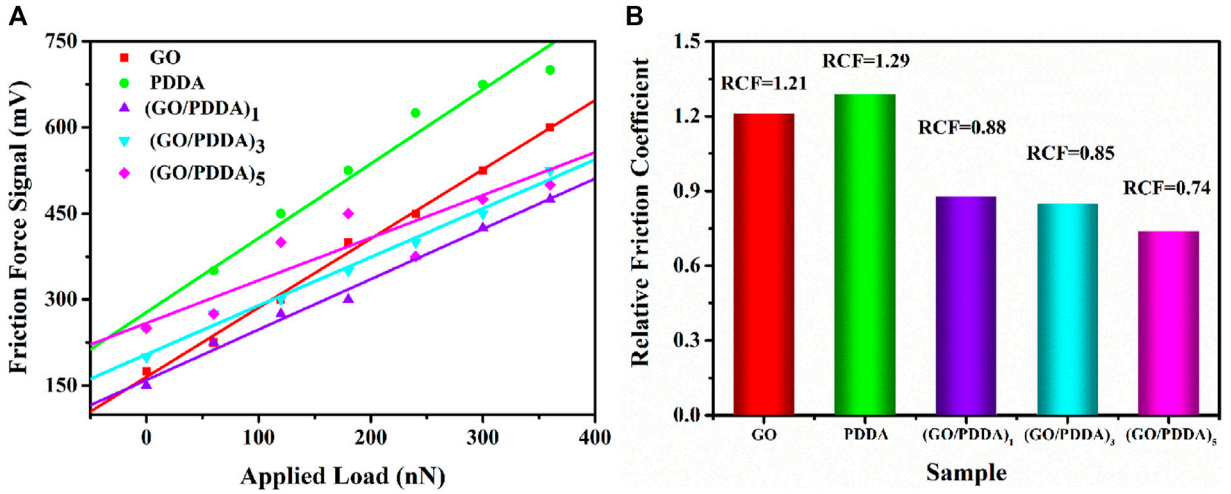

FIGURE 7 | (A) Friction force versus load curves and **(B)** relative friction coefficient for different samples.

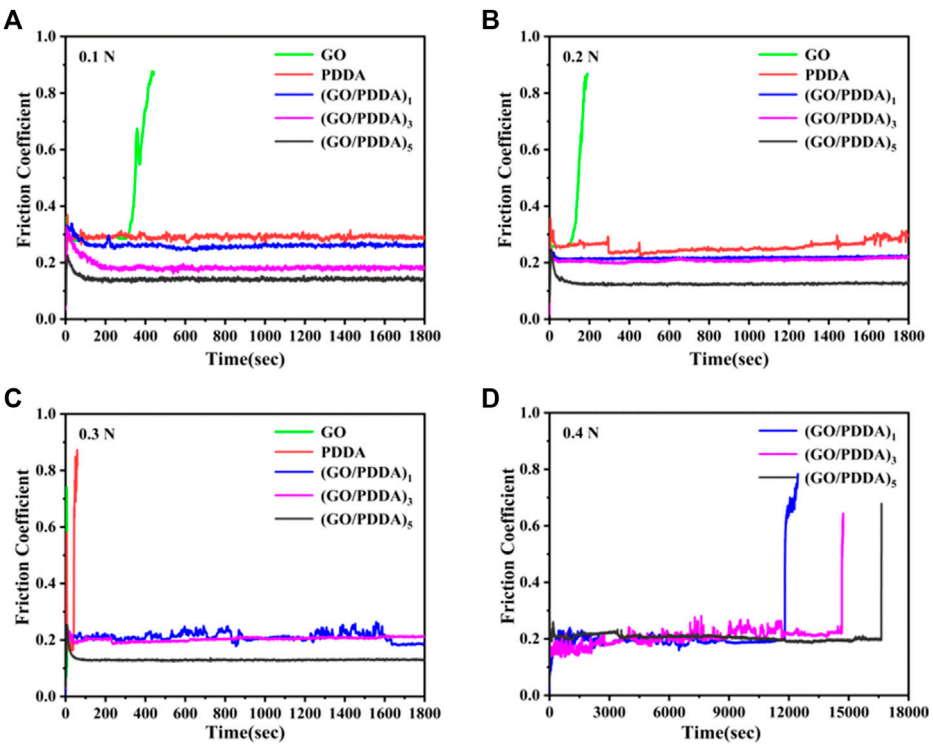

FIGURE 8 | Variation in friction coefficient with time for various sample at different applied loads and a sliding frequency of 1 Hz: **(A)** 0.1 N; **(B)** 0.2 N; **(C)** 0.3 N; **(D)** 0.4 N.

fabricate an elastic 3D crystal stack rather than a rigid 3D crystal stack composed of only GO sheets (Lee et al., 2015), which is a benefit to improve the anti-wear and load-carrying properties. Besides, a well-stacked GO–GO-layered structure was still maintained in $(GO/PDDA)_n$ layer (as mentioned in Raman analysis, **Figure 5**). The sliding phenomenon between the GO sheets is conducive to reducing friction coefficient. The sliding phenomenon appears to dominate as the number of $(GO/PDDA)_n$ layers increases, which causes a decrease in friction coefficient with increasing number of $(GO\text{-}PDDA)_n$ layers.

CONCLUSION

$(GO/PDDA)_n$ multilayer films with the topmost PDDA were constructed on hydroxylated silicon substrates by a LBL self-assembly method, where negatively charged GO sheets and positively charged PDDA were adsorbed alternately. The relationship between the microstructures and tribological behaviors of the films was studied. The results indicated that $(GO/PDDA)_n$ multilayer films exhibits excellent tribological behaviors at micro- and macroscale. Moreover, the film possesses better friction-reducing and anti-wear abilities with increasing number of $(GO\text{-}PDDA)_n$ layers. It could be attributed to the special structure in $(GO/PDDA)_n$ multilayer films. PDDA enlarge GO sheets to fabricate an elastic 3D crystal stack, which is a benefit to improve the anti-wear and load-carrying properties. Besides, a well-stacked GO–GO-layered structure was still maintained in the $(GO/PDDA)_n$ layer, which is conducive to reducing friction coefficient, and the microstructure enhanced with increasing number of $(GO\text{-}PDDA)_n$ layers. Therefore, such film structure is suitable to construct lubricant coatings for MEMS and other microdevices.

DATA AVAILABILITY STATEMENT

The original contributions presented in the study are included in the article/Supplementary Material. Further inquiries can be directed to the corresponding author.

AUTHOR CONTRIBUTIONS

JZ conceived and directed the project. LC and JZ designed the experiments. GW, YH, and CB prepared the samples and performed the material characterization. All authors contributed to analysis of the data and discussions of results. LC, YY, and JZ wrote the article with inputs from all authors.

ACKNOWLEDGMENTS

The authors gratefully acknowledge the National Natural Science Foundation of China (Grant No. 51765036) for financial support.

REFERENCES

Berman, D., Erdemir, A., and Sumant, A. V. (2014). Graphene: a New Emerging Lubricant. *Mater. Today* 17, 31–42. doi:10.1016/j.mattod.2013.12.003

Cao, X. a., Gan, X., Peng, Y., Wang, Y., Zeng, X., Lang, H., et al. (2018). An Ultra-low Frictional Interface Combining FDTS SAMs with Molybdenum Disulfide. *Nanoscale* 10, 378–385. doi:10.1039/c7nr06471c

Cassagneau, T., Guérin, F., and Fendler, J. H. (2000). Preparation and Characterization of Ultrathin Films Layer-By-Layer Self-Assembled from Graphite Oxide Nanoplatelets and Polymers. *Langmuir* 16, 7318–7324. doi:10.1021/la000442o

Chen, L., and Zhang, J. (2014). "Design and Properties of Self-Assembled Ordered Films for Nanolubrication," in *Surfactants in Tribology*. Editors G. Biresaw and K. L. Mittal (Boca Raton, Florida: CRC Press), 4, 97–150. doi:10.1201/b17691-9

Chen, L., Yang, B., and Zhang, J. (2014). Design and Evaluation of a Mixed Monolayer Consisting of Alkylsilane and Novel crown-type Molecules. *RSC Adv.* 4, 5213–5219. doi:10.1039/c3ra45690k

Chen, L., Li, N., Yang, B., and Zhang, J. (2016). Constructing High Load-Carrying Capacity Dual-Layer Film Assembled from Alkylsilane and Semi-spherical Molecules. *Microelectron. Eng.* 152, 1–5. doi:10.1016/j.mee.2015.12.010

Foster, T. T., Alexander, M. R., Leggett, G. J., and McAlpine, E. (2006). Friction Force Microscopy of Alkylphosphonic Acid and Carboxylic Acids Adsorbed on the Native Oxide of Aluminum. *Langmuir* 22, 9254–9259. doi:10.1021/la061082t

Guex, L. G., Sacchi, B., Peuvot, K. F., Andersson, R. L., Pourrahimi, A. M., Ström, V., et al. (2017). Experimental Review: Chemical Reduction of Graphene Oxide (GO) to Reduced Graphene Oxide (rGO) by Aqueous Chemistry. *Nanoscale* 9, 9562–9571. doi:10.1039/c7nr02943h

Houston, J. E., Doelling, C. M., Vanderlick, T. K., Hu, Y., Scoles, G., Wenzl, I., et al. (2005). Comparative Study of the Adhesion, Friction, and Mechanical Properties of CF3- and CH3-Terminated Alkanethiol Monolayers. *Langmuir* 21, 3926–3932. doi:10.1021/la046901t

Lee, C., Wei, X., Kysar, J. W., and Hone, J. (2008). Measurement of the Elastic Properties and Intrinsic Strength of Monolayer Graphene. *Science* 321, 385–388. doi:10.1126/science.1157996

Lee, H., Han, G., Kim, M., Ahn, H.-s., and Lee, H. (2015). High Mechanical and Tribological Stability of an Elastic Ultrathin Overcoating Layer for Flexible Silver Nanowire Films. *Adv. Mater.* 27, 2252–2259. doi:10.1002/adma.201405326

Li, P. F., Zhou, H., and Cheng, X.-H. (2013). Nano/micro Tribological Behaviors of a Self-Assembled Graphene Oxide Nanolayer on Ti/titanium alloy Substrates. *Appl. Surf. Sci.* 285, 937–944. doi:10.1016/j.apsusc.2013.09.019

Li, P., Liu, H., Chen, H., and Cheng, X. (2019). The Influence of APTES Interlayer on the Assembly and Tribological Properties of Graphene Coatings on Titanium Substrate. *Mater. Res. Express* 6, 016424–016429. doi:10.1088/2053-1591/ab2001

Liang, H., Bu, Y., Zhang, J., Cao, Z., and Liang, A. (2013). Graphene Oxide Film as Solid Lubricant. *ACS Appl. Mater. Inter.* 5, 6369–6375. doi:10.1021/am401495y

Liang, H., Bu, Y., Ding, J., and Zhang, J. (2015). A General Method for the Preparation of a Thickness-Controllable Fluoro-Containing Organic Film as a Solid Lubricant. *RSC Adv.* 5, 39884–39888. doi:10.1039/c5ra03900b

Liu, Y., Liu, P., Xiao, Y., and Luo, J. (2012). Investigation on Growth Process and Tribological Behavior of Mixed Alkylsilane Self-Assembled Molecular Films in Aqueous Solution. *Appl. Surf. Sci.* 258, 8533–8537. doi:10.1016/j.apsusc.2012.05.039

Maboudian, R., and Carraro, C. (2004). Surface Chemistry and Tribology of MEMS. *Annu. Rev. Phys. Chem.* 55, 35–54. doi:10.1146/annurev.physchem.55.091602.094445

Mi, Y., Wang, Z., Liu, X., Yang, S., Wang, H., Ou, J., et al. (2012). A Simple and Feasible Iin-Ssitu Reduction Route for Preparation of Graphene Lubricant Films Applied to a Variety of Substrates. *J. Mater. Chem.* 22, 8036–8042. doi:10.1039/c2jm16656a

Mungse, H. P., Tu, Y., Ichii, T., Utsunomiya, T., Sugimura, H., and Khatri, O. P. (2016). Self-assembly of Graphene Oxide on Silicon Substrate via Covalent Interaction: Low Friction and Remarkable Wear-Resistivity. *Adv. Mater. Inter.* 3, 1500410. doi:10.1002/admi.201500410

Ni, P., Li, H., Yang, M., He, X., Li, Y., and Liu, Z.-H. (2010). Study on the Assembling Reaction of Graphite Oxide Nanosheets and Polycations. *Carbon* 48, 2100–2105. doi:10.1016/j.carbon.2010.02.023

Ou, J., Wang, J., Liu, S., Zhou, J., and Yang, S. (2009). Self-assembly and Tribological Property of a Novel 3-layer Organic Film on Silicon Wafer with Polydopamine Coating as the Interlayer. *J. Phys. Chem. C* 113, 20429–20434. doi:10.1021/jp9073416

Ou, J., Wang, J., Liu, S., Mu, B., Ren, J., Wang, H., et al. (2010). Tribology Study of Reduced Graphene Oxide Sheets on Silicon Substrate Synthesized via Covalent Assembly. *Langmuir* 26, 15830–15836. doi:10.1021/la102862d

Ou, J., Wang, Y., Wang, J., Liu, S., Li, Z., and Yang, S. (2011). Self-assembly of Octadecyltrichlorosilane on Graphene Oxide and the Tribological Performances of the Resultant Film. *J. Phys. Chem. C* 115, 10080–10086. doi:10.1021/jp200597k

Ou, J., Liu, L., Wang, J., Wang, F., Xue, M., and Li, W. (2012). Fabrication and Tribological Investigation of a Novel Hydrophobic Polydopamine/graphene Oxide Multilayer Film. *Tribol. Lett.* 48, 407–415. doi:10.1007/s11249-012-0021-x

Popov, A. M., Lebedeva, I. V., Knizhnik, A. A., Lozovik, Y. E., and Potapkin, B. V. (2013). Structure, Energetic and Tribological Properties, and Possible Applications in Nanoelectromechanical Systems of Argon-Separated Double-Layer Graphene. *J. Phys. Chem. C* 117, 11428–11435. doi:10.1021/jp402765p

Porter, M. D., Bright, T. B., Allara, D. L., and Chidsey, C. E. D. (1987). Spontaneously Organized Molecular Assemblies. 4. Structural Characterization of N-Alkyl Thiol Monolayers on Gold by Optical Ellipsometry, Infrared Spectroscopy, and Electrochemistry. *J. Am. Chem. Soc.* 109, 3559–3568. doi:10.1021/ja00246a011

Qureshi, S. S., Zheng, Z., Sarwar, M. I., Félix, O., and Decher, G. (2013). Nanoprotective Layer-By-Layer Coatings with Epoxy Components for Enhancing Abrasion Resistance: toward Robust Multimaterial Nanoscale Films. *ACS Nano* 7, 9336–9344. doi:10.1021/nn4040298

Ramanathan, T., Abdala, A. A., Stankovich, S., Dikin, D. A., Herrera-Alonso, M., Piner, R. D., et al. (2008). Functionalized Graphene Sheets for Polymer Nanocomposites. *Nat. Nanotech.* 3, 327–331. doi:10.1038/nnano.2008.96

Shen, S., and Meng, Y. (2013). Effect of Surface Energy on the Wear Process of Bulk-Fabricated MEMS Devices. *Tribol. Lett.* 52, 213–221. doi:10.1007/s11249-013-0207-x

Song, S., Chu, R., Zhou, J., Yang, S., and Zhang, J. (2008). Formation and Tribology Study of Amide-Containing Stratified Self-Assembled Monolayers: Influences of the Underlayer Structure. *J. Phys. Chem. C* 112, 3805–3810. doi:10.1021/jp7100144

Stankovich, S., Dikin, D. A., Piner, R. D., Kohlhaas, K. A., Kleinhammes, A., Jia, Y., et al. (2007). Synthesis of Graphene-Based Nanosheets via Chemical Reduction of Exfoliated Graphite Oxide. *Carbon* 45, 1558–1565. doi:10.1016/j.carbon.2007.02.034

Tan, P., Dimovski, S., and Gogotsi, Y. (2004). Raman Scattering of Non-planar Graphite: Arched Edges, Polyhedral Crystals, Whiskers and Cones. *Phil. Trans. R. Soc. Lond. Ser. A: Math. Phys. Eng. Sci.* 362, 2289–2310. doi:10.1098/rsta.2004.1442

Tang, L., Wang, Y., Li, Y., Feng, H., Lu, J., and Li, J. (2009). Preparation, Structure, and Electrochemical Properties of Reduced Graphene Sheet Films. *Adv. Funct. Mater.* 19, 2782–2789. doi:10.1002/adfm.200900377

Yang, D., Velamakanni, A., Bozoklu, G., Park, S., Stoller, M., Piner, R. D., et al. (2009). Chemical Analysis of Graphene Oxide Films after Heat and Chemical Treatments by X-ray Photoelectron and Micro-raman Spectroscopy. *Carbon* 47, 145–152. doi:10.1016/j.carbon.2008.09.045

Conflict of Interest: The authors declare that the research was conducted in the absence of any commercial or financial relationships that could be construed as a potential conflict of interest.

Publisher's Note: All claims expressed in this article are solely those of the authors and do not necessarily represent those of their affiliated organizations, or those of the publisher, the editors, and the reviewers. Any product that may be evaluated in this article, or claim that may be made by its manufacturer, is not guaranteed or endorsed by the publisher.